

ARHDL Report 1

28 December 2006

Measurement of parent nuclides for (U-Th)/He chronometry by solution sector ICP-MS

Peter W. Reiners and Stefan Nicolescu

Department of Geosciences, University of Arizona, Tucson, AZ 85721

Index terms: *Geochronology, Thermochronology, Instruments and Techniques*

Keywords: *Analytical geochemistry, ICP-MS, (U-Th)/He, geochronology, thermochronology*

Please cite as:

Reiners, P.W. and Nicolescu, S. (2006), Measurement of parent nuclides for (U-Th)/He chronometry by solution sector ICP-MS, ARHDL Report 1,

<http://www.geo.arizona.edu/~reiners/arhdl/arhdl.htm>

7 September 2007:

Minor error in Figure 2 caption corrected. First sentence erroneously stated: "Figure 2. Measurements of $^{232}\text{Th}/^{229}\text{Th}$ and $^{238}\text{U}/^{233}\text{U}$ in "spiked normal" solutions, comprising either 25 or 50 μl of mixed ^{229}Th - ^{233}U spike and 50 μl of a mixed Th-U normal with 50 ng/ml U and 100 ng/ml Th."

Corrected: "Figure 2. Measurements of $^{232}\text{Th}/^{229}\text{Th}$ and $^{238}\text{U}/^{233}\text{U}$ in "spiked normal" solutions, comprising either 25 or 50 μl of mixed ^{229}Th - ^{233}U spike and 25 μl of a mixed Th-U normal with 50 ng/ml U and 100 ng/ml Th."

Abstract

(U-Th)/He chronometry requires accurate and precise measurement of U, Th, and in some cases, Sm, in analyzed phases. This is typically accomplished by dissolution and isotope dilution of the dated aliquot, and isotope ratio measurements of the resulting solution by inductively-coupled plasma mass spectrometry (ICP-MS). Here we present analytical procedures for these measurements using sector (high-resolution) ICP-MS, and analytical summaries of several thousand apatite and zircon samples and standards from our lab over approximately the last four years. These methods highlight current approaches and technical challenges in this part of (U-Th)/He chronometry, and also characterize U, Th, and Sm concentrations of these important accessory minerals across a wide range of rock types and locations. Analytical precision on U, Th, and Sm measurements is typically 0.1-1.0%, and precision on typical samples with more than ~10 pg of U and Th is usually better than 0.5%. Long-term reproducibility on spike calibrations is about 0.8-1.3% (one standard deviation over ~4.5 yr). Observed reproducibility of (U-Th)/He ages rarely approaches analytical precision (typically 2-3%, 2σ). Two standard deviations on replicate analyses of the commonly used standards Durango apatite and Fish Canyon Tuff (FCT) zircon are about 6% and 10%, respectively. Weighted mean ages and errors for these standards in our lab are 31.94 ± 0.17 Ma (95% confidence interval, with a 2σ required external error of 1.9 Ma or 5.9%, MSWD = 5.4, $n = 169$) for Durango apatite and 28.29 ± 0.26 Ma (95%; 2σ external error of 2.6 Ma or 9.3%, MSWD = 20, $n = 114$) for FCT zircon. Of all other samples in our compilation, approximately 50% of apatites have U and Th concentrations between 10 and 50 ppm and Sm concentrations between 100 and 300 ppm. In the vast majority of cases, ^{147}Sm contributions to ^4He in apatite will be greater than ~5% only when U concentrations are lower than about 5 ppm. Zircon samples show a broader range of U-Th concentrations, with U between 100 and 600 ppm in about 60% of zircons and Th between 50 and 200 ppm in about 50%.

Introduction

Thermochronology and geochronology based on accumulation and diffusion of radiogenic ^4He (e.g., Zeitler et al., 1987; Wolf et al., 1996; 1998; Farley, 2002) has proliferated in the last fifteen years. It is now widely applied in many tectonic and geomorphic studies, though work understanding its phenomenological bases and developing new analytical and interpretational approaches continues (e.g., Shuster and Farley, 2005; Shuster et al., 2006). Relatively high diffusivity of He in most minerals distinguishes (U-Th)/He dating as a low-temperature thermochronometer, useful in studies of shallow crustal exhumation, but it has also been used for estimating formation ages of materials formed at or near the surface (e.g., Shuster et al., 2005;

Blondes et al., 2007). At present, most (U-Th)/He (following historical usage, Sm is typically not included in the name of the technique) age measurements use a two stage analytical process involving first degassing an aliquot by heating it, and measuring its ^4He content by gas source mass spectrometry. This is followed by recovery and measurement of the parent nuclides in the same aliquot, usually by acid dissolution, spiking with a calibrated solution of parent nuclides with non-natural isotopic composition (isotope dilution), and measurement on an inductively-coupled plasma mass spectrometer (ICP-MS). Development of other analytical techniques for (U-Th)/He dating, including in-situ laser-ablation, is an active area of research. At the time of writing of this manuscript, laser ablation He dating has been shown to work for compositionally uniform monazite with extremely high U-Th concentrations and a very old He age (Boyce et al., 2006), and this general approach is promising for other minerals.

This paper has two general purposes. The first is to provide an overview of techniques and characterize protocols used by our lab over the last few years for measuring U, Th, and Sm contents of minerals commonly dated by the (U-Th)/He system by solution isotope dilution on a sector ICP-MS. In doing so we highlight a few technical issues and challenges associated with these measurements for both routine He dating and experimental developments. Analytical methods for and results of He analyses will be discussed in a forthcoming paper. The second purpose is to summarize typical concentrations and ranges of U, Th, and Sm concentrations in apatite and zircon from large body of data from approximately four years (2002-2006) of analyses in the (U-Th)/He Lab at Yale University, which is now at the University of Arizona. This compilation may be useful for other geochemical or geochronologic applications. Our approaches to measuring U, Th, and Sm have not necessarily emphasized achieving the highest precision or to exhaustively evaluate all potential sources of isotope ratio inaccuracies such as mass bias or isobaric interferences. Rather, we present our methods, accumulated data, and experience with this approach as a relatively efficient and high-sample throughput method for routine (U-Th)/He chronometry, which is adaptable to a wide range of phases. Other phases dated in our lab using techniques discussed here, with at least partial success, include titanite, garnet, magnetite, rutile, epidote, hibbonite, and biogenic apatite.

Sector ICP-MS

Sector ICP-MS (a.k.a. single-collector, high-resolution-ICP-MS, or HR-ICP-MS) is the method of choice for a wide range of inorganic trace and ultra-trace level concentration determination applications, but it is not widely used for geochronology. Most geochronology-related sector ICP-MS studies have focused on U-series isotopes (e.g., Hinrichs and Schnetger, 1999; Dorale et al.,

2001; Shen et al., 2002), although there is a growing interest in (U-Th)/Pb zircon dating (Tiepolo, 2003; Tiepolo et al., 2003; Chang et al., 2006). The lack of simultaneous multiple ion-counting in sector ICP-MS limits the precision of the isotope ratio determinations that are the fundamental basis of most geochronologic methods. However, relative to thermal ionization mass spectrometry and multi-collector ICP-MS, single-collector sector ICP-MS is inexpensive, technically straightforward, and capable of higher sample-throughput. For many geochronologic applications the ability to rapidly perform many analyses easily outweighs the disadvantages of lower precision (i.e., like certain types of cuisine, quantity has a quality all its own). Analytical precision also need not be significantly better than the actual reproducibility of replicate analyses, which for some thermochronologic applications is relatively poor (~2-4%, 1σ). Isotope dilution by sector ICP-MS is also capable of extremely low concentration U-Th (and, in some cases, Sm) determinations required for single-crystal apatite He dating, which is can be difficult for less sensitive quadrupole ICP-MS techniques.

Sector ICP-MS has been widely used for quantification of U (and to a lesser degree Th), and U isotope ratios, primarily in studies of anthropogenic contamination and human health (Kerl et al., 1997; Ting et al., 1999; Boulyga et al., 2000; Quétel et al., 2000; Boulyga and Becker, 2001; Pappas et al., 2002; Desideri et al., 2002; Krystek and Ritsema, 2002; Hinrichs et al., 2003; Gwiazda et al., 2004; Trešl et al., 2004). Analytical results and precision of these studies depend strongly on the application, but in general U-isotope ratios (e.g., $^{235}\text{U}/^{238}\text{U}$) can be measured to about 0.1% RSD, for solutions with about 1-100 ppt concentrations.

Analytical Methods

Because parent nuclide concentrations of individual crystals of accessory minerals can vary widely, even in the same centimeter-scale rock sample, parent and daughter measurements must be performed on the same aliquot. Single-crystal or, occasionally, multiple-crystal aliquots are heated *in vacuo* at ~900-1250 °C for several minutes to degas He, which is then spiked with ^3He , cryogenically (and/or via gettering) concentrated and purified, and quantified by isotope dilution and comparison to manometrically calibrated ^4He standards on a gas-source quadrupole mass spectrometer. Early analyses used resistance furnace for heating, but House et al. (2000) developed a method for laser heating of ~1 mm² Pt foils containing single apatite crystals, which has the advantage of significantly lower He blanks and greater sample throughput. Another great advantage of this method, at least for apatite, is that Pt foils can then be directly immersed in nitric acid and the grains inside dissolved for U-Th-Sm analysis without the often difficult task of transferring the degassed apatite crystal(s) from the foil to another vial.

For whole-grain (U-Th)/He dating, parent nuclide contents are measured by isotope dilution using solution ICP-MS. General preparation procedures used in our lab involved addition of isotopically distinctive U, Th, and Sm spikes to the crystal recovered and dissolved after degassing. Final solutions run on the ICP-MS were diluted to about 2-4 ml total volume, and are ~5-10% HNO₃, in some cases with ~0.5% HF. Concentrations of spike isotopes in resulting solutions were ~0.1-0.2 ppb, and the vast majority of natural U and Th concentrations were within 0.5-10 times these concentrations. In detail, different minerals require very different dissolution and dilution procedures. Our lab used nominally pure ²³³U, ²²⁹Th, and the enriched ¹⁴⁷Sm spike of Wasserburg et al. (1981), for spiking. Enriched uranium (²³⁵U) and ²³⁰Th can also be used as spikes.

Apatite

The simplest analytical procedure for U, Th, and Sm measurement, following the basics described by House et al. (2000), is that for apatite. Apatite can be dissolved directly from the Pt foil by addition of (in addition to the spike) even fairly dilute (~20%) nitric acid. In our experience, incomplete dissolution of apatite by this method is rare, although it has been observed in cases where Pt was heated by resistance furnace instead of by laser, possibly by metal deposition over openings of the Pt foil, and in cases of very large apatite aliquots. Another concern for apatite He dating in general is the potential for incomplete dissolution of U-Th-bearing inclusions in or on the crystals, which can lead to apparently unsupported He and “too-old” He ages. This potential is well-recognized and motivates careful screening processes during initial sample picking to exclude crystals with inclusions visible under plane-polarized and cross-polarized light at 120-160 times magnification. In some cases, small but high-U-Th inclusions may be difficult or impossible to detect by normal picking procedures (Farley and Stockli, 2002). Adoption of more aggressive dissolution procedures designed to attack refractory inclusions may recover U-Th and avoid the unsupported He problem, but in most cases resulting ages would still suffer from α -ejection correction inaccuracies caused by the inclusions (Farley et al., 1996; Hourigan et al., 2005).

In our lab, Pt foils with degassed apatite crystals were spiked with two different spike solutions, each in 5% HNO₃ solution. The first is 25 or 50 μ l of a nominally pure ²³³U-²²⁹Th spike with total U and Th concentrations of 7.55 ± 0.10 ng/ml and 12.3 ± 0.10 ng/ml respectively (uncertainties are long-term one standard deviations of all concentrations determined by spiking normal solutions of assumed known U-Th concentrations). The second is 25 or 50 μ l of an enriched (97%) ¹⁴⁷Sm spike with a total Sm concentration of 10.8 ± 0.10 ng/ml. Following

spiking, 200 μl of concentrated SeaStar Baseline HNO_3 is then added to each foil, and the mixture is heated at about 90 $^\circ\text{C}$ for two hours. After cooling, the solutions are diluted with 2.5 ml of double-distilled 18 M Ω H_2O , for final spike isotope concentrations of $\sim 0.1\text{-}0.2$ ppb.

Other minerals

Other phases require different dissolution techniques because they generally do not dissolve in nitric acid alone and require addition of HCl and/or HF. This cannot be performed in Pt foil, because HCl and HF dissolve considerable amounts of Pt, forming PtAr^+ complexes in the ICP-MS with isobaric interferences on U isotopes. In principle, $^{195}\text{Pt}^{40}\text{Ar}$ and $^{198}\text{Pt}^{40}\text{Ar}$ could be resolved from ^{235}U and ^{238}U using the high resolution mode on a sector ICP-MS, but the disadvantages of lower sensitivity, more difficult mass calibration, and triangular peak shape make avoidance of dissolved Pt in the solution a simpler option. House et al. (2000) used Pd foil for wrapping and laser-heating of titanite, and dissolved titanite directly from the foil in a spiked HCl-HF solution. In our experience however, this method dissolved large amounts of Pd that was difficult to keep in solution and appeared to produce unidentified interferences on U and Th. A more severe practical limitation was that the lower melting temperature made Pd foils more prone to melting or other damage during lasing, leading to relatively high probability of compromising quantitative recovery of the sample within it.

A possible solution to this for some minerals is to simply unwrap the Pt foil, transfer the naked grain(s) manually to a separate vial, and then spike and dissolve the sample there. This has several disadvantages however, not the least of which is the time required and risk of grain loss posed by the grain transfer process. Also, grains often fracture into several pieces or “sweat” during heating, leaving a residue inside the host Pt foil, which can be difficult or impossible to recover. Most importantly, it is difficult if not impossible to use this method to recover materials that break down into small fragments, powder, or melt during laser heating, as we have observed with garnet, epidote, fayalite, and other minerals.

To overcome these problems and insure dissolution of refractory inclusions, we routinely degassed grains of titanite, zircon, epidote, garnet, fayalite, magnetite, and other minerals in small $\sim 1\text{ mm}^2$ Nb foil envelopes, and subsequently dissolved the entire Nb foil and contents in Parr pressure digestion vessels (bombs). Foils with crystals were spiked with the same ^{233}U - ^{229}Th and ^{147}Sm spikes used for apatite, except that zircons and other high U-Th phases received larger spike doses. The foil and spike were mixed with 300 μl of HF and 50 μl of HNO_3 (both Seastar Baseline) in 0.35 ml Teflon “microvials,” inside a larger Teflon liner with nine other microvials and samples, 10 ml HF, and 0.42 ml HNO_3 (both Alfa Aesar Environmental Grade). Large Teflon

liners are bombed at 225 °C for 72 hours in 125 ml Parr bombs. After cooling, microvials are heated to dryness on an open hotplate, and then 300 µl of HCl (Seastar Baseline) is added. Microvials were then rebombed in the large Teflon liner containing 9 ml of HCl (Alfa Aesar Environmental Grade), at 200 °C for 24 hours. Rebombing in HCl is necessary to redissolve refractory fluoride salts. After cooling, microvials are again heated to dryness, and 200 µl of HNO₃ and 25 µl of HF (both Seastar Baseline grade) were added; capped microvials were gently heated for ~ 30 minutes, and then each sample was transferred to a larger Teflon vial, where it was diluted with double-distilled 18 MΩ H₂O to 3.225 ml of solution, at ~6% HNO₃ and 0.8% HF. For zircon, spike U-Th isotope concentrations are about 0.1-0.2 ppb, and about 80% of single crystal samples have natural U and Th concentrations within a factor of ~0.5-10.

A disadvantage of the Nb foil dissolution method is that sensitivity on U and Th peaks is decreased by about 35%, due to the large concentration of dissolved Nb in the solution. Also, although Nb is not routinely measured for other applications using our ICP-MS, it is possible that our Nb foil methods would result in high Nb blanks, were we to attempt to quantify this element in other samples using the same sample introduction equipment. For our purposes, the advantage of not needing to recover crystals or their residues following He extraction outweighs these disadvantages. Another note of caution regarding the use of Nb foil comes from using it with apatite. In several cases we have observed anomalous U-Th contents (particularly Th) of low-Th apatites dissolved with Nb foil. The problem is not observed with Durango apatite, possibly because the extremely high Th of Durango make it less susceptible. At this point the origin of this problem is unclear, but we do know that high resolution analyses on U and Th peaks do not indicate any significant amounts of isobaric interferences that may arise from species such as lanthanide-Nb complexes. In any case, at present we do not use or recommend dissolving and analyzing apatite crystals with Nb foil.

ICP-MS measurements

Instrumentation

All of the results shown here were performed on a Thermo Finnigan Element2, and most samples were processed with an all-PFA sample introduction assembly, including 100 µl/min. nebulizer, single-pass spray chamber, sapphire injector, and quartz torch. Nickel cones were used in all cases, to avoid PtAr interferences. All measurements were made in low resolution mode. Typical sensitivities on ²³⁸U for the range of operating conditions were between 1.2-2.0 x 10⁶ cps/ppb. For

each sample, including blanks and standards, the primary method measured ^{229}Th , ^{232}Th , ^{233}U , ^{235}U , and ^{238}U . For Sm measurements, a separate method measuring ^{147}Sm and ^{152}Sm was used, in order to avoid large mass jumps between measurements. Take-up times and wash times between samples were both 45 seconds. Wash solution was 6% HNO_3 between apatites, and 6% HNO_3 + 0.8% HF for zircons and other minerals with dissolved Nb.

Apatite samples were run with a method using EScan peak jumping with the magnet parked at mass 229.031, sample time of 2 ms, 100 samples per peak, mass and averaging windows of 5%, and counting mode, 5 runs and 400 passes for a total of 2000 isotope ratio measurements. Zircons were run with a similar method, except for 100% mass window, 15 samples per peak, 30% search window, 40% integration window, both analog and counting modes for ^{229}Th and ^{233}U , and 5 runs/150 passes for a total of 750 ratios. Methods employing either analog or counting modes were used on standards with a large range of U-Th concentrations to check the concordance of measured ratios for both detection modes. The Sm method for all samples was essentially the same as for U-Th on apatite, except magnet mass was set to 146.914.

Blank and calibration solutions

A typical ICP-MS measurement day for (U-Th)/He analyses processed about 50-100 samples prepared by the above methods. Each batch of analyses was accompanied by three to six sets of routine standards and blanks, used to check cleanliness of reagents and Teflon, spike concentrations and isotope ratios, and procedural blanks.

“Acid blanks” were mixed HNO_3 and H_2O , from which cps of U, Th, and Sm were used to check Teflon and reagent cleanliness. No spike is added to these blanks so quantitative determination of background U, Th, and Sm was not possible. On our Element2, which averaged $1.2\text{-}2.0 \times 10^6$ cps/ppb, we routinely observed about 100-300 cps for ^{232}Th and ^{238}U , and 1-10 cps for ^{229}Th , ^{233}U , and ^{235}U .

“Spike blanks” were the same as acid blanks (5% HNO_3 solutions) except with a 25 or 50 μl shot of ^{233}U - ^{229}Th spike or ^{147}Sm spike. Besides being an additional check on U-Th-Sm in the reagents and Teflonware, measured $^{238}\text{U}/^{233}\text{U}$, $^{232}\text{Th}/^{229}\text{Th}$, and $^{152}\text{Sm}/^{147}\text{Sm}$ of spike blanks were used to define isotopic abundances used in isotope dilution calculations for concentrations of U, Th, and Sm in the spikes and unknowns run on the same day. Spike blanks run between February 2002 through July 2006 (Fig. 1) yield apparent ^{233}U and ^{229}Th atomic abundances in the spikes of 0.9955 ± 0.0024 , and 0.9973 ± 0.0030 (uncertainties as one standard deviations). Anomalously impure spike isotope ratios measured near analysis number 60 (Fig. 1) were traced to Teflon vials

with cracks on the interior surfaces, which presumably trapped U-Th from previous analyses that was not removed by normal boiling-acid washing procedures.

“Spiked norms” contain 1.25 ng and 2.50 ng of natural U and Th, respectively, with either 25 or 50 μl of ^{233}U - ^{229}Th spike. A second type of spiked norm contains 1.25 ng of natural Sm, with 25 μl of ^{147}Sm spike. Measured $^{238}\text{U}/^{233}\text{U}$, $^{232}\text{Th}/^{229}\text{Th}$, and $^{152}\text{Sm}/^{147}\text{Sm}$ ratios of these spiked norms, together with ratios measured on spike blanks, are used to calculate the concentration of U, Th, and Sm in the spikes. Average ratios of three to six spiked norm samples run each analytical session over the last several years are shown in Figure 2. Relative standard deviations (RSD) on isotope ratio measurements of individual spiked norms is typically $<0.5\%$. Long-term reproducibility of spiked norms for the period of November 2003 through July 2006, when a single stock solution was being used, are 0.83% for $^{232}\text{Th}/^{229}\text{Th}$ and 1.3% for $^{238}\text{U}/^{233}\text{U}$ (Fig. 2b). This reproducibility probably reflects a fundamental limit to manual pipetting precision, as well as periodic evaporative concentration of the spike solution, as described below.

A significant time-systematic variation in spiked norm ratios that reflects changing spike concentration was observed between about June and November of 2003 (Fig. 2a). During this time, measured $^{238}\text{U}/^{233}\text{U}$ and $^{232}\text{Th}/^{229}\text{Th}$ both decreased by about 7-9%. No trend was observed in spike blank ratios over this period. This period corresponds to decreasing volume of the U-Th spikes, from about 15 to about 3-5 ml due to consumption. At this time the volumes of stock U-Th normals remained constant at about 1000 ml. The decreasing ratios were likely caused by evaporative concentration of ^{233}U and ^{229}Th in the remaining small volumes of spike. This demonstrates the importance of routine calibrations of spike concentration by this method. Suggestions of episodic trends of decreasing spiked norm ratios on the order of 1.5-2.0% are also observed on shorter timescales between November 2003 and July 2006. These trends are also likely due to evaporation of spike solution from the 30 ml spike vial used for routine spiking, because each trend is punctuated by episodes of restocking of the 30 ml spike vial from a much larger (1 liter) bottle.

“Platinum blanks” and “Nb blanks” are empty Pt or Nb foil packets processed in exactly the same way as normal apatite or zircon (or other phases requiring bomb dissolution) samples, respectively. These same foils are also heated by laser, to determine ^4He blanks during degassing. Platinum blanks average 0.6 ± 0.4 pg U and 1.0 ± 0.2 pg Th (uncertainties as 1σ standard error) (Fig. 3). Niobium blanks are about four to ten times higher than Pt blanks, averaging 2.6 ± 0.5 pg U and 5.5 ± 1.0 pg Th (Fig. 3). Sm blanks are similar to those of Th.

“Bomb blanks” are procedural blanks for dissolutions requiring Parr “bombing.” They are processed the same way as Nb blanks, but without Nb foil. Bomb blanks are indistinguishable from Nb blanks, averaging 2.7 ± 0.5 pg U and 5.7 ± 1.1 pg Th (Fig. 3).

Apatite

Figure 4 shows U and Th contents of approximately 3000 dated apatite (and other phosphate) aliquots, plotted against %RSD on measured $^{238}\text{U}/^{233}\text{U}$ and $^{232}\text{Th}/^{229}\text{Th}$ ratios. The majority of these analyses are on single apatite crystals from plutonic or sedimentary rocks. Approximately 200 are from basement rocks of the Washington Cascades, and approximately 200 are from turbidites of the Northern Apennines; others are from miscellaneous unknowns, Durango apatite standards, meteoritic phosphates, and biogenic apatite. The data form a broad inverse correlation with increasing RSD on measured isotope ratios with decreasing U and Th contents. The vast majority of these data, especially those with masses of U or Th greater than 0.01 ng, have RSD less than 0.5%. For reference, 0.01 ng would be the mass of U in an apatite with a c-axis perpendicular half-width (radius) of 75 μm , aspect ratio of 2.5, and U concentration of about 0.5 ppm.

Parent and daughter nuclide measurements for (U-Th)/He dating are made on the same aliquots, so ages are based on molar contents, not concentrations, of U, Th, and He. Nonetheless, U and Th concentrations of dated grains can be estimated from careful measurements of crystal dimensions in digital photomicrographs, which are required for α -ejection corrections. Typically, c-axis-parallel and perpendicular dimensions of apatite crystals are measured in at least two different orientations rotated 90° about the c-axis, and an idealized hexagonal prism geometry is assumed to estimate the crystal volume. Assuming an apatite density of 3.1 g/cm^3 , the crystal mass, and therefore U and Th concentrations, are estimated. This is not routinely performed for apatites with highly irregular morphologies, such as irregular shards of larger crystals characteristic of the widely used Durango apatite standard, or some apatites plucked from fission-track mounts.

Figure 5 shows U and Th concentrations of apatites estimated by the above procedures. It is not clear to what extent these concentrations can be considered an accurate reflection of U and Th concentrations in natural igneous apatites as a whole, because of various sampling biases inevitably resulting from selection of both rocks and individual crystals suitable for dating. Nevertheless, these data suggest that typical igneous apatites have Th/U ~ 1.2 to 4, and that roughly 5-10% of apatites have more than 100 ppm U, $\sim 20\%$ have U between 50-100 ppm, $\sim 20\%$ have U between 25-50 ppm, and roughly half less than 25 ppm.

Samarium in apatite

In zircon, Sm is rarely if ever present in concentrations sufficient to contribute significantly to radiogenic He and age. Apatite, however, shows a much wider range of Sm concentration, and, more importantly, Sm/U and Sm/Th ratios. Figure 6 shows the proportion of an apatite He age (roughly the proportion of ^4He) derived from ^{147}Sm . The majority of Durango aliquots have Sm contributions between 0.3-0.4%. Other apatites show as little as 0.03% to as much as 70% Sm-derived He contributions, though the vast majority of samples lie between 0.1 and 3.0%. Not surprisingly, the proportion of He derived from Sm shows a strong negative correlation with both U and eU ($U + 0.235\text{Th}$) concentration (Fig. 6b). If the relationship in Figure 6b holds true for most apatites, it suggests that in the vast majority of cases, Sm will contribute more than ~5% of radiogenic He only for apatites with less than ~5 ppm U. Interestingly, in this dataset all of the apatites with more than 10% Sm-derived ^4He are from two different types of rocks: oceanic gabbros, and granitoids within or adjacent to fault zones. The latter suggest a potentially important role for fluid mobility of parent nuclides in apatites in such settings.

Zircon

Figure 7 shows U and Th contents of approximately 1200 single-crystal (or crystal fragment) zircon aliquots, plotted against %RSD on measured $^{238}\text{U}/^{233}\text{U}$ and $^{232}\text{Th}/^{229}\text{Th}$ ratios. Approximately 110 of these are from zircons from the quickly cooled Fish Canyon Tuff, a widely used age standard for U/Pb (Schmitz et al., 2001) and (U-Th)/He dating. Others are from miscellaneous locations and rock types; many are detrital. In contrast to apatite, there is very little indication of an inverse correlation between RSD on measured isotope ratios and U and Th contents. This suggests that some other factor, most like quantity of dissolved Nb, which lowers sensitivity on U and Th, may be limiting measurement precision. Nevertheless, RSDs are similar to those of apatite, albeit at higher average U-Th contents.

Uranium and Th concentrations of dated zircons can be estimated from crystal dimension measurements performed in analogous ways as for apatite, assuming tetragonal prism or tetragonal prism with bipyramidal terminations crystal morphologies, and a zircon density of 4.6 g/cm^3 (e.g., Reiners et al., 2005). As with apatites, U-Th concentrations of several types of gem-quality zircons, dated as irregular fragments of much larger crystals (Nasdala et al., 2004), could not be reliably estimated and are not shown here. Figure 8 shows U and Th concentrations of zircons estimated by these methods. As with apatite, there are potential biases in this compilation resulting from grain and sample selection procedures, but many of these grains were detrital,

sampling a broad range of rock types and ages, so some estimate of “typical” crustal zircon U and Th concentrations can be made.

PtAr and $^{238}\text{U}/^{235}\text{U}$

One advantage of using ^{233}U , rather than ^{235}U , as a spike in U isotope dilution is that, at least for samples with sufficient U concentrations, it permits measurement of $^{238}\text{U}/^{235}\text{U}$. Using our procedures, which are not necessarily designed to maximize precision, typical RSD on this measured ratio is about 1-5%. In principle, this could be used to monitor and correct for instrumental mass bias, which, in the mass range of U and Th, can be as large as 0.5-1.0 %/amu, based on other measured isotope ratios. Whereas mass fractionation in quadrupole instruments generally favors higher mass isotopes, several additional phenomena in sector instruments have the potential to induce a reverse mass fractionation (Quétel et al., 2000). As a result it is not clear in which direction from 137.88 the $^{238}\text{U}/^{235}\text{U}$ would be expected to shift as a result of mass bias, but monitoring of this ratio has the potential to correct for such effects. In our experience however, the measured intensity ratio of masses 238 and 235 is much more strongly affected by PtAr interference than by mass bias.

House et al. (2000) indicated that no Pt was dissolved by their procedure involving dissolution of grains *in situ* from Pt foil, and we have not observed visible macroscopic evidence of Pt foil dissolution in any of our apatite analyses. However, we have observed significant and occasionally extremely large (10^7 - 10^8 cps) peaks in the 190-198 amu range with the characteristic isotopic abundance pattern of Pt, in all apatite solutions in which we have looked for them. Zircons also show considerable dissolved Pt, though not typically as large as in apatite. The HNO_3 used to dissolve apatite from Pt foil should not dissolve the Pt, but it is possible that small amounts of F and/or Cl in the apatite itself produces HF and/or HCl in solution that dissolves Pt. This is supported by our observations that dissolved apatite samples have much higher Pt (and PtAr) peaks than Pt blanks processed with the same acids and procedures. Durango apatite, for example, can have $2\text{-}3 \times 10^6$ cps on masses 194, 195, and 196, whereas Pt blanks typically have $3\text{-}4 \times 10^4$ cps on the same peaks.

This dissolved Pt produces a significant PtAr peak at mass 235 and, to a lesser degree, at mass 238, interfering with ^{235}U and ^{238}U in low resolution. Because ^{195}Pt is 4.7 times more abundant than ^{198}Pt , and ^{235}U is 138 times less abundant than ^{238}U , a small amount of dissolved Pt can dramatically decrease the measured (238/235). Because interference of $^{195}\text{Pt}^{40}\text{Ar}$ on mass 235 also means there is some interference of $^{198}\text{Pt}^{40}\text{Ar}$ on mass 238, this could potentially signify an

erroneous (238/233) measurement, and erroneously high $^{238}\text{U}/^{233}\text{U}$, which would complicate U concentration determinations. Assuming all deviation of measured 238/235 from 137.88 is due to PtAr interference, the ratio of actual $^{238}\text{U}/^{233}\text{U}$ to measured (238/233) of a sample, as a function of the measured (235/238), is:

$$\frac{\left(\frac{^{238}\text{U}}{^{233}\text{U}}\right)_{\text{real}}}{\left(\frac{238}{233}\right)_m} = \frac{\left[1 - \frac{^{198}\text{Pt}^{40}\text{Ar}}{^{195}\text{Pt}^{40}\text{Ar}} \left(\frac{235}{238}\right)_m\right]}{\left[1 - \frac{^{198}\text{Pt}^{40}\text{Ar}}{^{195}\text{Pt}^{40}\text{Ar}} \left(\frac{^{235}\text{U}}{^{238}\text{U}}\right)\right]}$$

where $(238/233)_m$ and $(235/238)_m$ are the measured intensity ratios for those masses, and $(^{235}\text{U}/^{238}\text{U})$ is the expected U isotopic ratio (1/137.88). Figure 9 shows the magnitude of this effect, as a function of measured (238/235). The measured (238/233) is only 0.5% different from the “true” $^{238}\text{U}/^{233}\text{U}$ ratio when the measured (238/235) is 32, or 77% lower than the natural $^{238}\text{U}/^{235}\text{U}$. Thus the measured (238/235) can be significantly different from the natural $^{238}\text{U}/^{235}\text{U}$, with extremely little effect on the U concentration determination, which is based on (238/233).

Figure 10 shows measured (238/235) of apatite and zircon solutions, as a function of U content of the solution. Most samples with more than ~0.5-1.0 ng of U have (238/235) close to 137.88. With lower U contents, measured (238/235) shows a broad sigmoidal decrease. Trends of predicted (238/235) for constant assumed intensities of 1.5, 15, and 150 cps at mass 238 from $^{198}\text{Pt}^{40}\text{Ar}$ (and proportional cps at 235 from $^{195}\text{Pt}^{40}\text{Ar}$) for different U contents (assuming a sensitivity of 1.5×10^6 /ppb, and a standard sample volume of 3 ml) match the observed trend well. Assuming a typical sensitivity of 1.5×10^6 cps/ppb, the $^{198}\text{Pt}^{40}\text{Ar}$ intensities shown in Figure 10 would imply effective “concentrations” of 0.1 ppt to 1.0 ppq $^{198}\text{Pt}^{40}\text{Ar}$. It is difficult to use these results to constrain the proportion of Pt that forms PtAr or the concentration of dissolved Pt in our procedures, because we do not routinely measure Pt. However, analysis of Pt and PtAr peaks in acid blanks and Pt blanks suggests a PtAr/Pt ratio of approximately 10^{-4} . For the effective PtAr “concentrations” assumed above in modeling decreasing (238/235) with decreasing U content, this would correspond to total dissolved Pt concentrations of about 0.01 – 1.0 ppb ^{198}Pt .

It is also possible that PtAr may have a source not in every analyzed solution, but in sample introduction materials in the ICP-MS from previous high-Pt samples. Support for this comes from the fact that zircon and apatite samples follow roughly similar trends in Fig. 9, despite the fact that most zircons are processed without Pt (a subset with low (238/235) at

relatively high U contents were plucked from Pt foil following degassing, which probably resulted in dissolution of some adhered Pt). Alternatively, a small amount of Pt may reside in Teflon used for dissolutions. We have found that boiling in aqua regia is the only effective way to remove dissolved metals such as Nb and Pt from Teflon, although it is possible that a very small amount of Pt remains in the Teflon after this procedure. In any case, the good news is that monitoring for the (238/235) in analyzed samples serves as an extremely sensitive test for the presence of dissolved Pt that could potentially compromise U measurements. The bad news is that because this ratio is so sensitive to even minute amounts of Pt, it does not permit effective correction for mass fractionation by measuring $^{238}\text{U}/^{235}\text{U}$.

(U-Th)/He Ages

Standards

It is beyond the scope of this paper to discuss the He measurements that complement U, Th, and Sm measurements for (U-Th)/He dating, but propagated analytical uncertainties for most typical apatite and zircon samples lead to an estimated analytical uncertainty on (U-Th)/He ages of approximately 1-3% (1σ). In some cases, reproducibility of multiple aliquots approaches analytical uncertainty. For example, eight analyses of single crystal zircons from a xenolith erupted from a basaltic vent average 157 ka with one standard deviation of 4 ka (2.6%) (Blondes et al., 2007), and fourteen chips of large gem quality crystals of Sri Lanka zircon average 442 Ma with one standard deviation of 10 Ma (2.3%) (Nasdala et al., 2004). In general, however, reproducibility of repeat analyses of (U-Th)/He ages is significantly worse than analytical precision. Cooling ages of apatite and zircon from igneous rocks typically show scatter on the order of one standard deviation of at least 6%, and in many cases more than 10%. This has several possible origins, including variable He diffusion characteristics among grains, unidentified intracrystalline inclusions that prevent complete U-Th-Sm recovery following degassing, or petrographic siting effects such as He implantation from adjacent high-U-Th phases or varying He retention due to varying diffusivity or partitioning of surrounding phases. It is likely, however, that a major origin of the observed poor reproducibility comes through uncertainty in the alpha-ejection correction (Farley et al., 1996). Most of this uncertainty probably does not come from uncertainty in actual dimensions of dated grains, which is typically only a few percent (e.g., Farley, 2002). Instead it arises through uncertainties in relating observed grain boundaries of dated aliquots to original boundaries in the host rock, implantation from other

phases, and inhomogeneous distribution of parent nuclides in dated grains (Farley et al., 1996; Reiners et al., 2004; Hourigan et al., 2005). It is extremely difficult to estimate, *a priori*, the expected magnitude of error arising from any of these potential sources. Thus He ages typically show a much greater scatter and higher MSWD than expected based on analytical precision alone.

Figure 11 shows 169 age determinations on small (~20-200 μm) fragments of much larger (~2-3 cm) gem-quality crystals of Durango apatite. Durango apatite, while useful as an analytical standard, is atypical of normal apatites, especially in its high Th/U (~15-22). Replicate aliquots of this standard yield an average age of 31.9 Ma, with two standard deviations of 2.2 Ma (6.6%), and a weighted mean age and error of 31.94 ± 0.17 Ma (95% confidence interval, with a 2σ required external error of 1.9 Ma or 5.9%, MSWD = 5.4). This mean age is within error of, but slightly older than, the 31.4 ± 0.5 (2σ) weighted mean of K/Ar ages of feldspars from volcanic rocks bracketing the Durango apatite deposit (Naeser and Fleischer, 1975) and recalculated using Steiger and Jager's (1977) decay constants (Green, 1985). Green (1985) favored an even younger (but still within error) fission-track age for Durango of 30.8 ± 1.7 (2σ) Ma. More recent measurements by McDowell et al. (2004) yielded a bracket age from $^{40}\text{Ar}/^{39}\text{Ar}$ analyses of 31.44 ± 0.18 (2σ), and 24 (U-Th)/He ages with a mean age of 31.02 with two standard deviations of 2.0 Ma. The reason for the slightly older age obtained from our compilation is unknown, but lack of Sm measurements in about one-third of the analyses may contribute. Sm typically has the effect of reducing the (U-Th)/He age by about 0.3-0.5% in Durango apatite (although two aliquots appear to have Sm age contributions of ~1% and 5%, with reasonable ages). The observed external error on Durango apatite cannot have an origin in alpha-ejection correction, as these grains are small chips of much larger crystals, but U-Th heterogeneity probably still contributes to He heterogeneity and separation of parent and daughters, and therefore age irreproducibility (Boyce and Hodges, 2005).

Figure 11 shows (U-Th)/He ages of Fish Canyon Tuff (FCT) zircon, another commonly used volcanic age standard. Schmitz et al. (2001) obtained high precision U/Pb zircon ages on the FCT of 28.48 ± 0.06 (2σ) Ma, and other high precision zircon U/Pb studies yield similar results (e.g., Bachman et al., 2007). There is evidence suggesting that some zircon growth significantly preceded eruption, however, and Bachman et al. (2007) suggest an eruption age of 28.04 ± 0.18 (2σ) Ma, based on Renne et al.'s (1998) sanidine $^{40}\text{Ar}/^{39}\text{Ar}$ ages, based on the fact that this system would remain open at magmatic, pre-eruption temperatures. One hundred fourteen single grain (U-Th)/He zircon ages average 28.3 Ma, with two standard deviations of 2.8 Ma, and mean age

and errors of 28.29 ± 0.26 Ma (95%; 2σ external error of 2.6 Ma or 9.3%, MSWD = 20). The observed external error probably has a component in errors associated with the effects of heterogeneous intracrystalline U-Th distribution on the α -ejection correction. Laser ablation depth profiling of FCT zircons show a range of U-Th zonation styles and extents that should lead to an approximately 10% scatter in ages from this effect alone (Hourigan et al., 2005).

Conclusions and future developments

Uranium, Th, and Sm measurement by isotope dilution using sector ICP-MS provides routine precision on parent nuclides for single crystal apatite and zircon (U-Th)/He dating on the order of 0.1-0.5%. Typical procedural blanks for apatite are about 0.6 pg U and 1.0 pg Th, and for zircon (Parr bomb dissolution) are about 2-3 pg U and 5-6 pg Th. Routine dissolution of single crystals from Pt or Nb foils used for He extraction allow recovery of the same aliquot that was degassed, and results do not indicate loss (e.g., through volatilization) of parent nuclides. Although better precision on measured isotope ratios and therefore U-Th-Sm contents of dated aliquots is possible in some cases, other sources of uncertainty in (U-Th)/He dating that are difficult to quantify *a priori* currently limit the precision of the technique, so improved parent nuclide precision is not a high priority. The greatest benefits of sector ICP-MS for this dating technique are the high sample-throughput and precision significantly below the typically observed ~6-10% reproducibility (two standard deviations) of (U-Th)/He ages.

Because of the relatively recent resurrection of (U-Th)/He chronometry, both interpretational and analytical aspects of the method are evolving rapidly. Sector ICP-MS used with laser ablation sampling in particular poses a number of potential benefits currently being developed, including in complementary zircon U/Pb dating (Tiepolo, 2003; Tiepolo et al., 2003), and apatite fission-track dating (Hasebe et al., 2004; Donelick et al., 2005) in the same grains. For both methods, LA-ICP-MS shows considerable potential not only for increased sample throughput, but also for understanding relationships between chronologic and chemical characteristics of crystals (e.g., Black et al., 2004). Laser ablation ICP-MS may also find utility in relating crystal chemistry and (U-Th)/He ages, especially in partially reset samples, which frequently show poor grain-to-grain reproducibility, the origins of which are not well understood.

A potentially powerful practical benefit of LA-ICP-MS in (U-Th)/He dating is the ability to measure the intracrystalline distribution of U and Th in crystals prior to dating them. This is important because the typically applied α -ejection correction assumes uniform U-Th distribution,

whereas some types of zonation involving strongly contrasting U-Th concentrations in crystal interiors and their ~ 20 μm rims, can lead to age inaccuracies as high as $\sim 35\%$ (Farley et al., 1996; Reiners et al., 2004; Hourigan et al., 2005). Extents and styles of U-Th zonation can vary dramatically from crystal-to-crystal, even within a single hand specimen, so single-crystal characterization is necessary. Uranium-Th zonation in ~ 30 to 100 μm deep rim-to-core pits drilled by LA-ICP-MS have been used to develop crystal-specific α -ejection corrections that dramatically improve the precision and accuracy of ages on problematically zoned samples (Hourigan et al., 2005).

Measurement of U-Th zonation by LA-ICP-MS depth profiling can also be combined with U/Pb dating, to provide both U/Pb and (U-Th)/He ages on dated crystals (Rahl et al., 2003; Reiners et al., 2005). Under certain conditions, this method can also resolve distinct U/Pb ages of subcrystalline domains such as metamorphic overgrowths on older igneous cores. Combined with subsequent (U-Th)/He dating of the grain (minus the ~ 30 μm diameter laser ablation pit), these methods essentially provide three different ages in the life of a zircon: crystallization, metamorphism, and exhumation (Campbell et al., 2005).

Finally, another possible use of LA-ICP-MS in (U-Th)/He chronometry that has received little attention thus far but poses perhaps the greatest potential, is measurement of both He and U-Th contents by laser ablation within single crystals (e.g., Boyce et al., 2006). Although current techniques involve two separate measurement steps and sub-crystal-domain aliquots (because at present no technique can measure both U-Th and He contents in the same ablated volume) further development of this procedure would lead to at least two significant advances. First, it would allow for much higher sample throughput, aiding detrital thermochronology studies requiring many dated crystals. Second, it could potentially resolve intracrystalline variations in (U-Th)/He age caused by slow cooling and diffusive He loss. Rather than calculation of a bulk age corresponding to the whole crystal and its effective closure temperature (Dodson, 1973), a series of ages, from core to rim, could be calculated, corresponding to a closure profile (Dodson, 1986). Rather than a single time-temperature point in the rock's thermal history, the closure profile could be inverted to model a finite time-temperature path, as in some types of routine $^{40}\text{Ar}/^{39}\text{Ar}$ dating (McDougall and Harrison, 1999) and $^4\text{He}/^3\text{He}$ thermochronology (Shuster and Farley, 2005).

Acknowledgments

We thank Bruce Nelson and Mihai Ducea for providing us with ^{233}U and ^{147}Sm spikes, respectively. We thank Torsten Lindemann and Sean Thompson for helpful analytical and instrumental advice. Several basic aspects of the procedures described here were developed in Ken Farley's research group at Caltech prior to 1999, though misapplications or misinterpretations presented here are the responsibility of the authors alone. This work was supported by NSF grant EAR 0236965 to PWR.

References

- Bachman, O, Oberli, F., Dungan, M.A., Meier, M, Mundil, R., and Fischer, H. (2007), $^{40}\text{Ar}/^{39}\text{Ar}$ and U–Pb dating of the Fish Canyon magmatic system, San Juan Volcanic field Colorado: Evidence for an extended crystallization history, *Chem. Geol.*, *236*, 134-166.
- Black, L.P., Kamo, S.L., Allen, C.M., Davis, D.W., Aleinikoff, J.N., Valley, J.W., Mundil, R., Campbell, I.H., Korsch, R.J., Williams, I.S., and Foudoulis, C. (2004), Improved $^{206}\text{Pb}/^{238}\text{U}$ microprobe geochronology by the monitoring of a trace-element-related matrix effect; SHRIMP, ID-TIMS, ELA-ICP-MS and oxygen isotope documentation for a series of zircon standards, *Chem. Geol.*, *205*, 115-140.
- Blondes, M.B., Reiners, P.W., Edwards, B.R., and Biscontinini, A.E. (2007), Dating young basalts by (U-Th)/He on xenolithic zircons, *Geology*, *35*, 17-20.
- Boulyga, S.F., and Becker, J.S. (2001), Determination of uranium isotopic composition and ^{236}U content of soil samples and hot particles using inductively coupled plasma mass spectrometry, *Fres. J. Analyt. Chem.*, *370*, 612-617.
- Boulyga, S.F., Becker, J.S., Dietze, H.-J., and Matusevich, Z.H. (2000), Isotope ratio measurements of spent reactor uranium in the environmental samples using inductively coupled plasma mass spectrometry, *Int. J. Mass Spec.*, *203*, 143-154.
- Boyce, J.W., and Hodges, K.V. (2005), U and Th zoning in Cerro de Mercado (Durango, Mexico) fluorapatite: Insights regarding the impact of recoil redistribution of radiogenic ^4He on (U–Th)/He thermochronology, *Chem. Geol.*, *219*, 261-274.
- Boyce, J.W., Hodges, K.V., Olszewski, W.J., Jercinovic, M.J., Carpenter, B., and Reiners, P.W. (2006), Laser microprobe (U-Th)/He geochronology, *Geochim. Cosmochim. Acta*, *70*, 3031-3039.
- Campbell, I.H., Reiners, P.W., Allen, C.M., Nicolescu, S., and Upadhyay, R. (2005), He-Pb double dating of detrital zircons from the Ganges and Indus Rivers: Implications for sediment recycling and provenance studies, *Earth Planet. Sci. Lett.*, *237*, 402-432.
- Chang, Z., Vervoort, J.D., McClelland, W.C., and Knaack, C. (2006), U/Pb dating of zircon by LA-ICP-MS, *Geochem. Geophys. Geosyst.*, *7*, Q05009, doi:10.1029/2005GC001100.
- Desideri, D., Meli, M.A., Roselli, C., Testa, C., Boulyga, S.F., and Becker, J.S. (2002), Determination of ^{236}U and transuranium elements in depleted uranium ammunition by α -spectrometry and ICP–MS, *Analy. Bioanalyt. Chem.*, *374*, 1091–1095.
- Dodson, M.H. (1973), Closure temperature in cooling geochronological and petrological systems, *Contrib. Mineral. Petrol.*, *40*, 259-274.
- Dodson, M.H. (1986), Closure profiles in cooling systems, *Materials Science Forum*, *7*, 145-154.

- Donelick, R.A., O'Sullivan, P.B., and Ketcham, R.A. (2005), Apatite Fission-Track Analysis, in *Low-Temperature Thermochronology: Techniques, Interpretations, and Applications*, *Rev. Mineral. Geochem.*, vol. 58, edited by P.W. Reiners and T.A. Ehlers, pp. 49-94, MSA, Chantilly, VA.
- Dorale, J.A., Edwards, R.L., Alexander Jr., E.C., Shen, C.C., Richards, D.A., and Cheng, H. (2001), *Uranium-series dating of speleothems: Current techniques, limits, & applications*, in *Studies of Cave Sediments*, edited by J. Mylroie and I.D. Sasowsky, Kluwer Academic/Plenum, New York.
- Farley, K.A. (2002), (U-Th)/He dating: Techniques, calibrations, and applications, in *Noble Gases in Geochemistry and Cosmochemistry*, *Rev. Mineral. Geochem.*, vol. 47, edited by D. Porcelli, C.J. Ballentine, and R. Wieler, pp. 819-844, MSA, Chantilly, VA.
- Farley, K.A., and Stockli, D.F. (2002), (U-Th)/He dating of phosphates: apatite, monazite, and xenotime. in *Phosphates: Geochemical, Geobiological, and Materials Importance*, *Rev. Mineral. Geochem.*, vol. 48, edited by M.J. Kohn, J. Rakovan, and J.M. Hughes, pp. 559-577. MSA, Chantilly, VA.
- Farley, K.A., Wolf, R.A., and Silver, L.T. (1996), The effects of long alpha-stopping distances on (U-Th)/He ages, *Geochim. Cosmochim. Acta*, 60, 4223-4229.
- Green, P.F. (1985), Comparison of zeta calibration baselines for fission-track dating of apatite, zircon, and sphene, *Chem Geol.*, 58, 1-22.
- Gwiazda, R.H., Squibb, K., McDiarmid, M., and Smith, D. (2004), Detection of depleted uranium in urine of veterans from the 1991 Gulf War, *Health Phys.*, 86, 12-18.
- Hasebe, N., Barbarand, J., Jarvis, K., Carter, A., and Hurford, A.J. (2004), Apatite fission-track chronometry using laser ablation ICP-MS, *Chem Geol.*, 207, 135-145.
- Hinrichs, J., Hamester M., Lindemann T., and Wills, J.D. (2003), Detection of ultra-trace levels of uranium in urine with sector-field ICPMS: Quantification and isotope ratio determination, *Inter. Labmate*, 28, 98-99.
- Hinrichs, J., and Schnetger, B. (1999), A fast method for the simultaneous determination of ^{230}Th , ^{234}U and ^{235}U with isotope dilution sector field ICP-MS, *Analyst*, 124, 927-932.
- Hourigan, J.K., Reiners, P.W., and Brandon, M.T. (2005), U-Th zonation-dependent alpha-ejection in (U-Th)/He chronometry, *Geochim. Cosmochim. Acta*, 69, 3349-3365.
- House, M.A., Farley, K.A., and Stockli, D.F. (2000), He chronometry of apatite and titanite using Nd-YAG laser heating, *Earth Planet. Sci. Lett.*, 183, 365-368.
- Jonckheere, R., Mars, M., Van den haute, P., Rebetz, M., and Chambaudet, A. (1993), L'apatite de Durango (Mexique): Analyse d'un minéral standard pour la datation par traces de fission, *Chem Geol.*, 103, 141-154.
- Kerl, W., Becker J.S., Dietze H.-J., and Dannecke, W. (1997), Isotopic and ultratrace analysis of uranium by double-focusing sector field ICP mass spectrometry. *Fres. J. Analyt. Chem.*, 359, 407-409.
- Krystek P., and Ritsema, R. (2002), Determination of uranium in urine - measurement of isotope ratios and quantification by use of inductively coupled plasma mass spectrometry, *Analyt. Bioanayt. Chem.*, 374, 226-229.
- Ludwig, K.R. (2003), User's Manual for Isoplot 3.00, *Berkely Geochronology Center Special Publication No. 4*, Berkeley, CA, 70 pp.
- McDougall, I. and Harrison, T.M. (1999), *Geochronology and Thermochronology by the $^{40}\text{Ar}/^{39}\text{Ar}$ Method*, 2nd ed., 269 pp., Oxford Univ. Press.
- McDowell, F.W., McIntosh, W.C., and Farley, K.A. (2005), A precise ^{40}Ar - ^{39}Ar reference age for the Durango apatite (U-Th)/He and fission-track dating standard, *Chem. Geol.*, 214, 249-263.
- Naeser, C.W., and Fleischer, R.L. (1975), Age of the apatite at Cerro de Mercado, Mexico: A problem for fission track annealing corrections, *Geophys. Res. Lett.*, 2, 67-70.

- Nasdala, L., Reiners, P.W., Garver, J.I., Kennedy, A.K., Stern, R.A., Balan, E., and Wirth, R. (2004), Incomplete retention of radiation damage in zircon from Sri Lanka, *Am. Mineral.*, *89*, 219-231.
- Pappas, R.S., Ting, B.G., Jarrett, J.M., Paschal, D.C., Caudill, S.P., and Miller, P.T. (2002), Determination of uranium-235, uranium-238 and thorium-232 in urine by magnetic sector inductively coupled plasma mass spectrometry, *J. Analyt. Atomic Spec.*, *17*, 131-134.
- Quétel, C.R., Vogl, J., Prohaska, T., Nelms, S., Taylor, P.D.P., and de Bièvre, P. (2000), Comparative performance study of ICP mass spectrometers by means of U isotopic measurements, *Fres. J. Analyt. Chem.*, *368*, 148-155.
- Rahl, J.M., Reiners, P.W., Campbell, I.H., Nicolescu, S., Allen, C.M. (2003), Combined single-grain (U-Th)/He and U/Pb dating of detrital zircons from the Navajo Sandstone, Utah, *Geology*, *31*, 761-764.
- Reiners, P.W. (2005), Zircon (U-Th)/He Thermochronometry, in *Low-Temperature Thermochronology: Techniques, Interpretations, and Applications*, *Rev. Mineral. Geochem.*, vol. 58, edited by P.W. Reiners and T.A. Ehlers, pp. 151-176, MSA, Chantilly, VA.
- Reiners, P.W., Spell, T.L., Nicolescu, S., and Zanetti, K.A. (2004), Zircon (U-Th)/He thermochronometry: He diffusion and comparisons with $^{40}\text{Ar}/^{39}\text{Ar}$ dating, *Geochim. Cosmochim. Acta*, *68*, 1857-1887.
- Renne, P.R., Swisher, C.C., Deino, A.L., Karner, D.B., Owens, T.L., and DePaolo, D.J. (1998), Intercalibration of standards, absolute ages and uncertainties in $^{40}\text{Ar}/^{39}\text{Ar}$ dating, *Chem. Geol.*, *145*, 117-152.
- Schmitz, M.D. and Bowring, S.A. (2001), U-Pb zircon and titanite systematics of the Fish Canyon Tuff: an assessment of high precision U-Pb geochronology and its application to young volcanic rocks, *Geochim. Cosmochim. Acta*, *65*, 2571-2587.
- Shen, C.C., Edwards, R.L., Cheng, H., Dorale, J.A., Thomas, R.B., Moran, S.B., Weinstein, S.E., and Edwards, H.N. (2002), Uranium and thorium isotopic and concentration measurements by magnetic sector inductively coupled plasma mass spectrometry, *Chem. Geol.*, *185*, 165-178.
- Shuster, D.L., and Farley, K.A. (2005), $^4\text{He}/^3\text{He}$ Thermochronometry: Theory, Practice, and Potential Complications, in *Low-Temperature Thermochronology: Techniques, Interpretations, and Applications*, *Rev. Mineral. Geochem.*, vol. 58, edited by P.W. Reiners and T.A. Ehlers, pp. 181-203, MSA, Chantilly, VA.
- Shuster, D.L., Flowers, R.M., and Farley, K.A. (2006), The influence of natural radiation damage on helium diffusion kinetics in apatite, *Earth Planet. Sci. Lett.*, *249*, 148-161.
- Shuster, D.L., Vasconcelos, P.M., Heim, J.A., and Farley, K.A. (2005), Weathering geochronology by (U-Th)/He dating of goethite, *Geochim. Cosmochim. Acta*, *69*, 659-673.
- Steiger, R.H., and Jager, E. (1977), Subcommittee on geochronology. Convention on the use of decay constants in geo- and cosmochronology, *Earth Planet. Sci. Lett.* *36*, 359-362.
- Tiepolo, M. (2003), In situ Pb geochronology of zircon with laser ablation-inductively coupled plasma-sector field mass spectrometry, *Chem. Geol.*, *199*, 159-177.
- Tiepolo, M., Bottazzi, P., Palenzona, M., and Vannucci, R. (2003), A laser probe coupled with ICP-double-focusing sector-field mass spectrometer for in situ analysis of geological samples and U-Pb dating of zircon, *Can. Mineral.*, *41*, 259-272.
- Ting, W., Paschal, D.C., Jarrett, J.M., Pirkle, J.L., Jackson, R.J., Sampson, E.J., Miller, D.T., and Caudill, S.P. (1999), Uranium and thorium in urine of United States residents: Reference range concentrations, *Environ. Res. Sect. A*, *81*, 45-51.
- Trešl, I., Wannemacker, G.D., Quétel, C.R., Petrov, I., Vanhaecke, F., Moens, L., and Taylor, P.D.P., (2004), Validated measurements of the uranium isotopic signature in human urine

- samples using magnetic sector-field Inductively Coupled Plasma Mass Spectrometry, *Environ. Sci. Technol.*, 38, 581-586.
- Wasserburg, G.J., Jacobsen, S.B., DePaolo, D.J., McCulloch, M.T., and Wen, T. (1981), Precise determination of Sm/Nd ratios, Sm and Nd isotopic abundances in standard solutions, *Geochim. Cosmochim. Acta*, 45, 2311-2323.
- Wolf, R.A., Farley, K.A., and Silver, L.T. (1996), Helium diffusion and low-temperature thermochronometry of apatite, *Geochim. Cosmochim. Acta*, 60, 4231-4240.
- Wolf, R.A., Farley, K.A., and Kass, D.M. (1998), Modeling of the temperature sensitivity of the apatite (U-Th)/He thermochronometer, *Chem. Geol.* 148, 105-114.
- Zeitler, P.K., Herczeg, A.L., McDougall, I., and Honda, M. (1987), U-Th-He dating of apatite: a potential thermochronometer, *Geochim. Cosmochim. Acta* 51, 2865-2868.

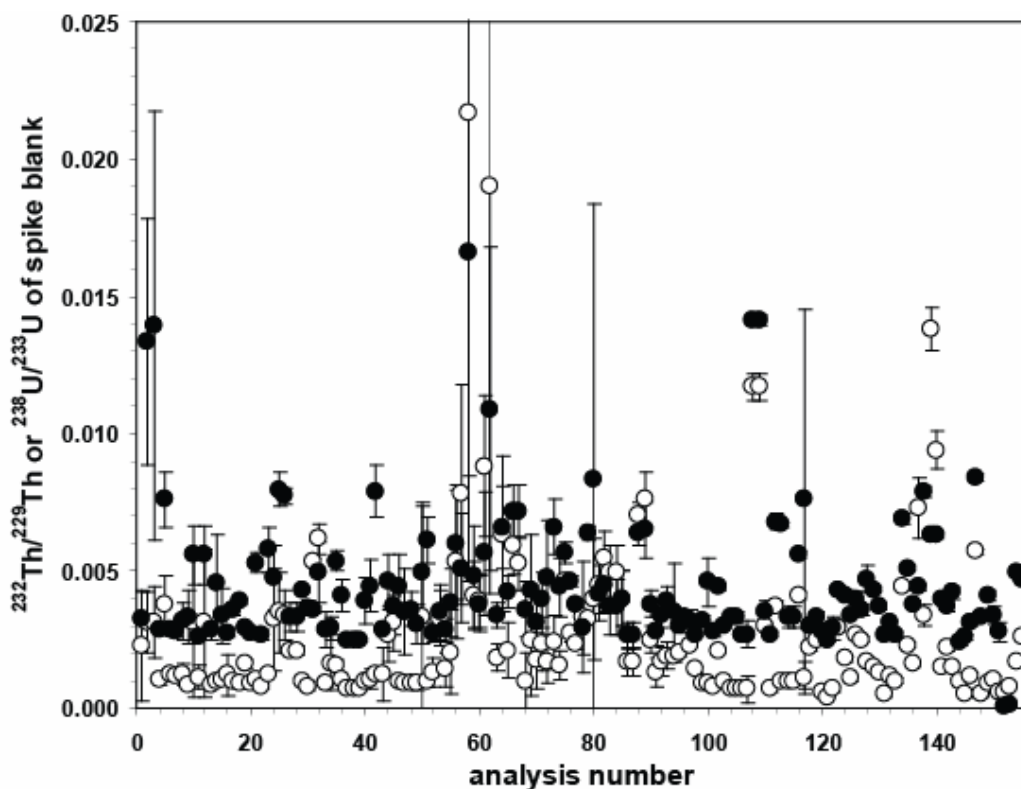


Figure 1. Apparent fractional impurity of ^{229}Th (open circles) and ^{233}U (filled circles) in spike as measured by “spike blanks” in routine analyses from February 2002 through July 2006. Error bars are 1 standard deviation of multiple replicates (typically 3-6) in each analytical run covering a sample batch. Lower analysis numbers are more recent. Spike blanks comprise either 25 or 50 μl of mixed ^{229}Th - ^{233}U spike (in concentrations of Th: 12.3 ng/ml; U: 7.55 ng/ml), in 2-4 ml 5% HNO_3 . Measured spike blank isotopic abundances are used in isotope dilution calculations. Anomalous impure spike isotope ratios near analysis number 60 were traced to cracked Teflon vials that presumably were not adequately cleaned by normal boiling acid washing procedures.

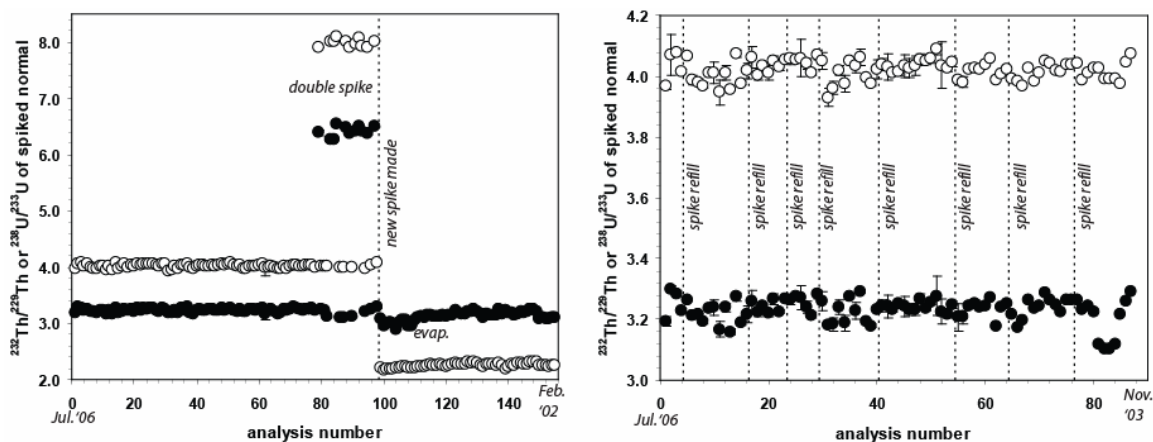


Figure 2. Measurements of $^{232}\text{Th}/^{229}\text{Th}$ and $^{238}\text{U}/^{233}\text{U}$ in “spiked normal” solutions, comprising either 25 or 50 μl of mixed ^{229}Th - ^{233}U spike and 25 μl of a mixed Th-U normal with 50 ng/ml U and 100 ng/ml Th. Uranium and Th in the normal solution have natural isotopic ratios (most commercially available U normals are depleted in ^{235}U). Large volumes of normal solutions are maintained in order to mitigate against evaporative concentration changes with time, and new normals are periodically prepared from new certified solutions. Spike concentrations for use in isotope dilution calculations are calibrated for each analysis batch from measured spiked normal ratios, assuming accurate and precise normal concentrations and volumes delivered to the spiked normal solutions. This approach allows for correction of changing spike concentration (e.g., due to evaporative concentration) over time. Evaporative concentration of spike solution can be seen in the steady decline in spiked normal isotope ratios between analysis numbers 120 and 98 (left panel), and between spike refill episodes in analysis sequence in the right panel. Long-term day-to-day reproducibility of spiked normal ratios (and therefore changes in apparent spike concentration) is 0.83 and 1.3% (1σ) for Th and U, respectively.

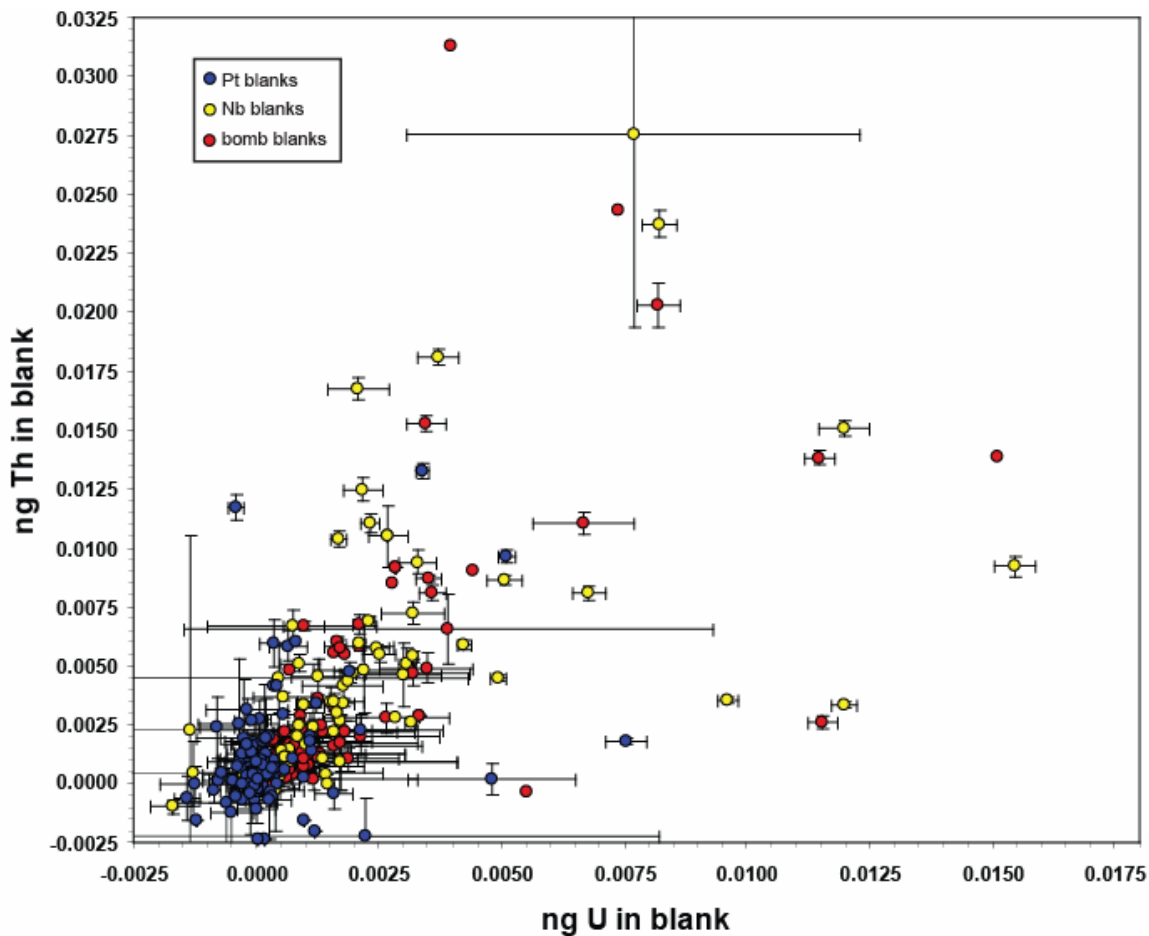


Figure 3. Procedural Th and U blanks for apatite and zircon U-Th dissolution and measurement methods. Apparent blank values can be slightly less than zero if the procedural blank has a lower $^{238}\text{U}/^{233}\text{U}$ or $^{232}\text{Th}/^{229}\text{Th}$ than the spike blank for that analytical run. Platinum blanks are empty Pt foils processed in the same way as apatite samples (spiking and dissolution in nitric acid). Niobium blanks are similar but for zircon methods (spiking and dissolution in hydrofluoric and nitric acid in Parr bombs, followed by re-bombing in hydrochloric acid, followed by re-dissolution in nitric and hydrofluoric acid). Bomb blanks are similar to Nb blanks, but without the Nb foil. Blanks occasionally show apparent negative U and/or Th concentrations because they can have measured $^{232}\text{Th}/^{229}\text{Th}$ or $^{238}\text{U}/^{233}\text{U}$ ratios slightly less than those of the spike blanks. Points without error bars are samples for which uncertainty estimations were not available, but they are similar to those of other samples. Platinum blanks average 0.6 ± 0.4 pg U and 1.0 ± 0.2 pg Th (uncertainties as 1σ standard error); Nb blanks average 2.6 ± 0.5 pg U and 5.5 ± 1.0 pg Th; bomb blanks average 2.7 ± 0.5 pg U and 5.7 ± 1.1 pg Th.

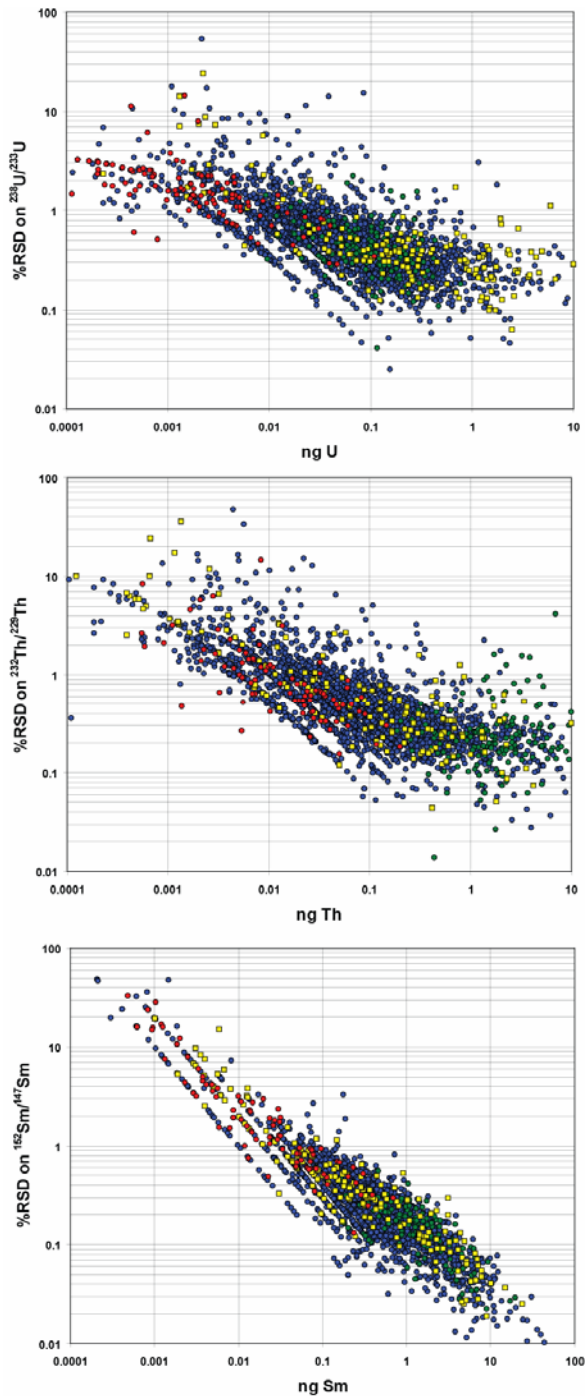


Figure 4. Percent relative standard deviation (RSD) on measured $^{238}\text{U}/^{233}\text{U}$, $^{232}\text{Th}/^{229}\text{Th}$, and $^{152}\text{Sm}/^{147}\text{Sm}$ (natural to spike isotope ratios) for approximately 2600 igneous and metamorphic apatite specimens (blue circles), 136 meteoritic phosphates (apatite and whitlockite; red circles), 170 Durango apatite specimens (green circles), and 173 biogenic apatite specimens (conodonts and fossil tooth enamel (yellow squares)). Sm ratios are for approximately one-third as many specimens, because Sm was not measured in our lab until relatively recently. Highly linear trends at low %RSD (seen especially in Sm) are artifacts caused by rounding of RSD digits by ICP-MS software.

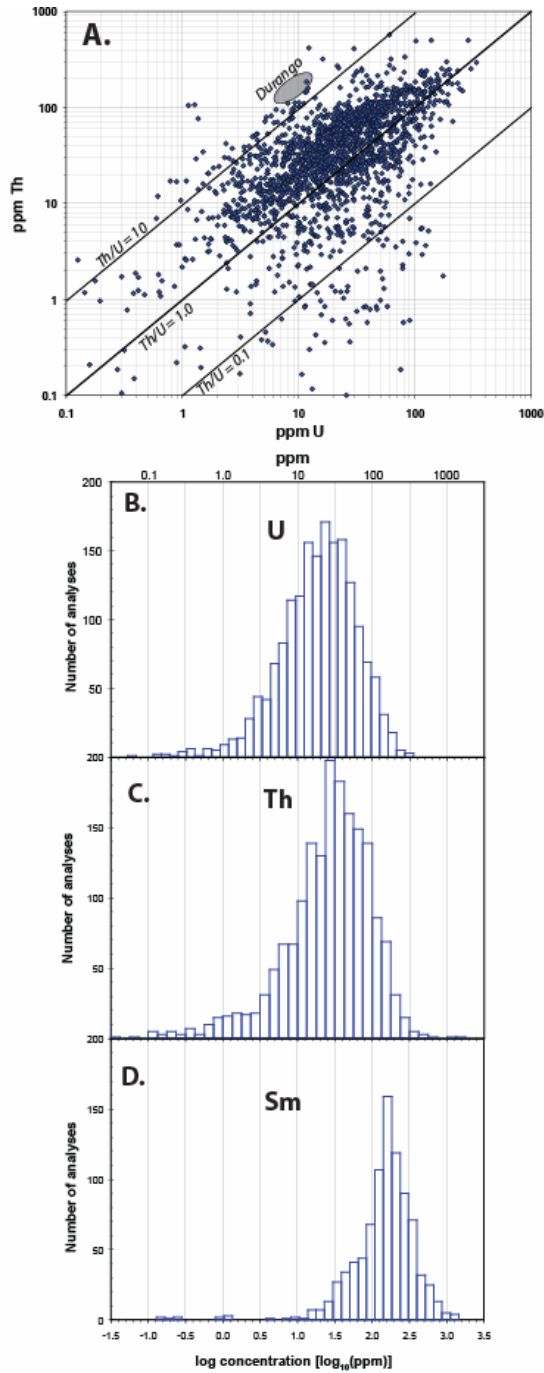


Figure 5. **A.** Concentrations of U and Th in approximately 1800 dated apatite aliquots (mostly single crystals) calculated from measured U and Th contents and estimated volumes and densities of dated crystals. Only samples with typical cylindrical morphologies are shown, because the volumes of irregularly shaped grains are not routinely measured, thus masses (required for concentration determinations) are not estimated. Durango apatite concentrations are approximate, because mass and therefore concentrations, are not routinely measured for these irregular fragments of larger crystals. **B-D.** Histograms of log concentrations for U, Th, and Sm.

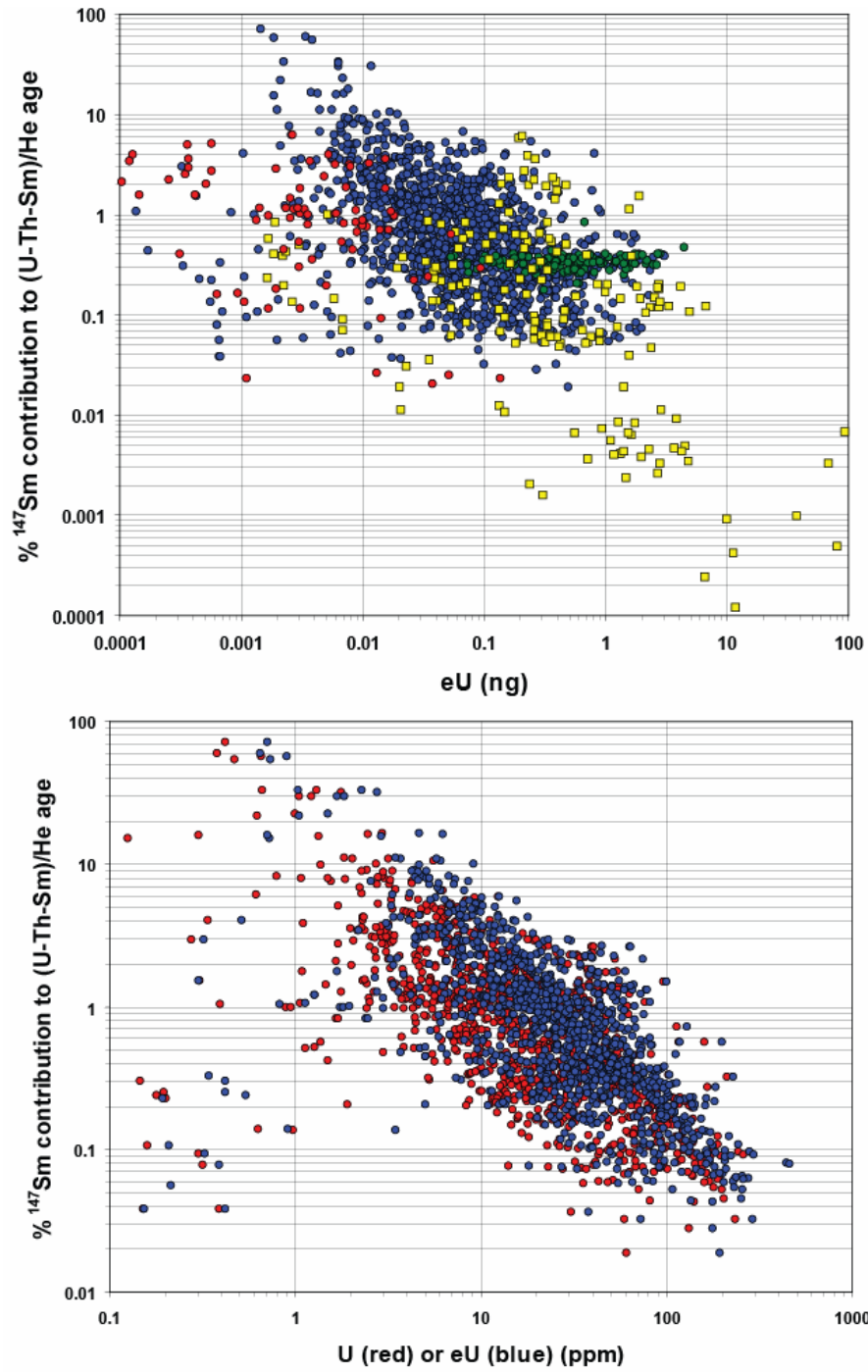


Figure 6. Percent age (or ⁴He) contribution from ¹⁴⁷Sm, as a function of eU (U+0.235Th) as either total mass (**A**) and concentration (**B**). Panel **B** also plots points as a function of U concentration alone, for reference. In panel A, symbols are as in Fig. 4. Durango apatite have 0.2-0.5% Sm-derived He. The lower panel suggests that, in general, Sm will contribute 5% or more to the He age only for apatites with less than ~ 5 ppm U.

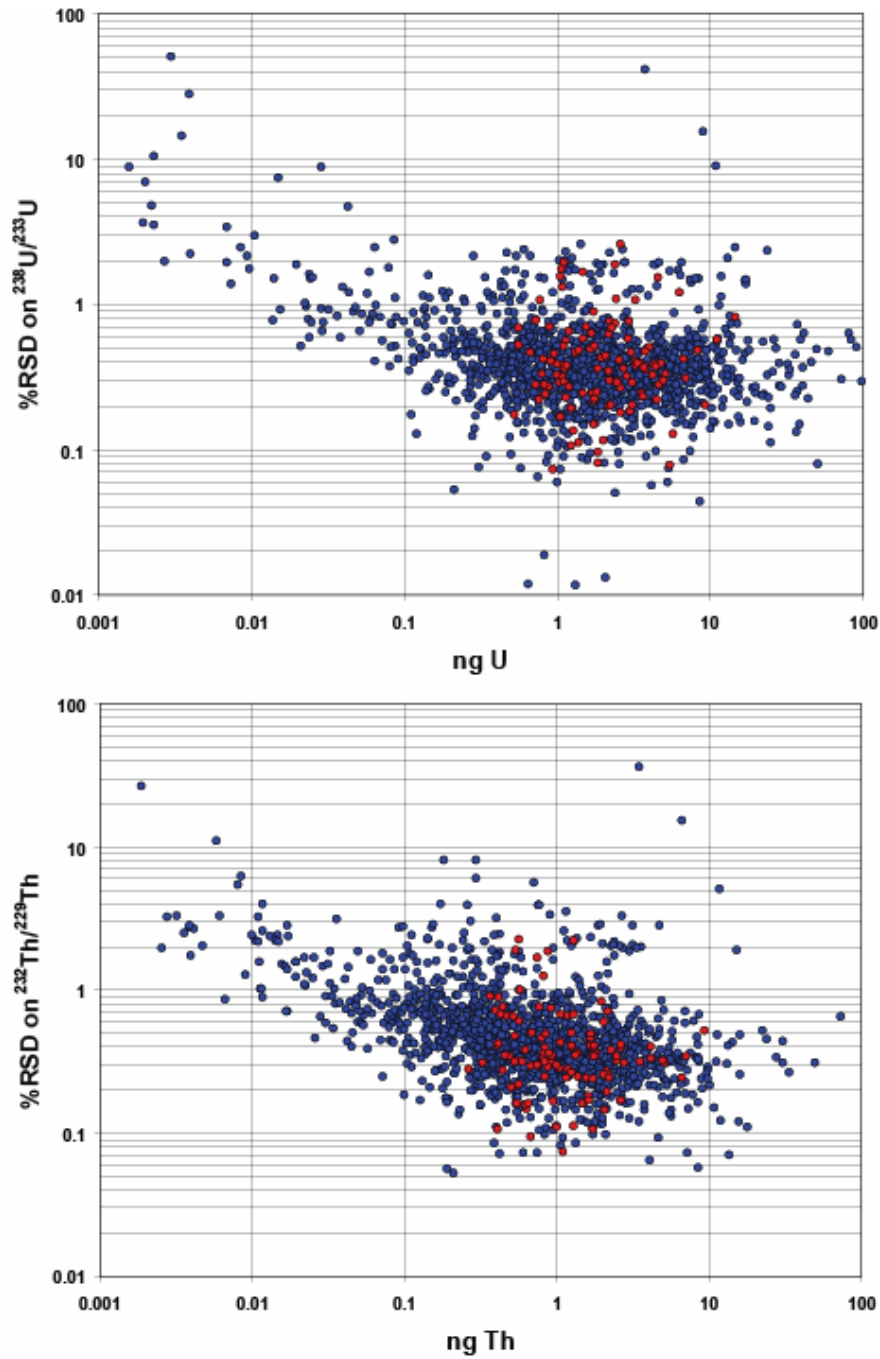


Figure 7. Percent RSD on measured $^{238}\text{U}/^{233}\text{U}$ and $^{232}\text{Th}/^{229}\text{Th}$ (natural to spike isotope ratios) for approximately 1200 zircon aliquots. Red circles: zircons from Fish Canyon Tuff; blue circles: other samples.

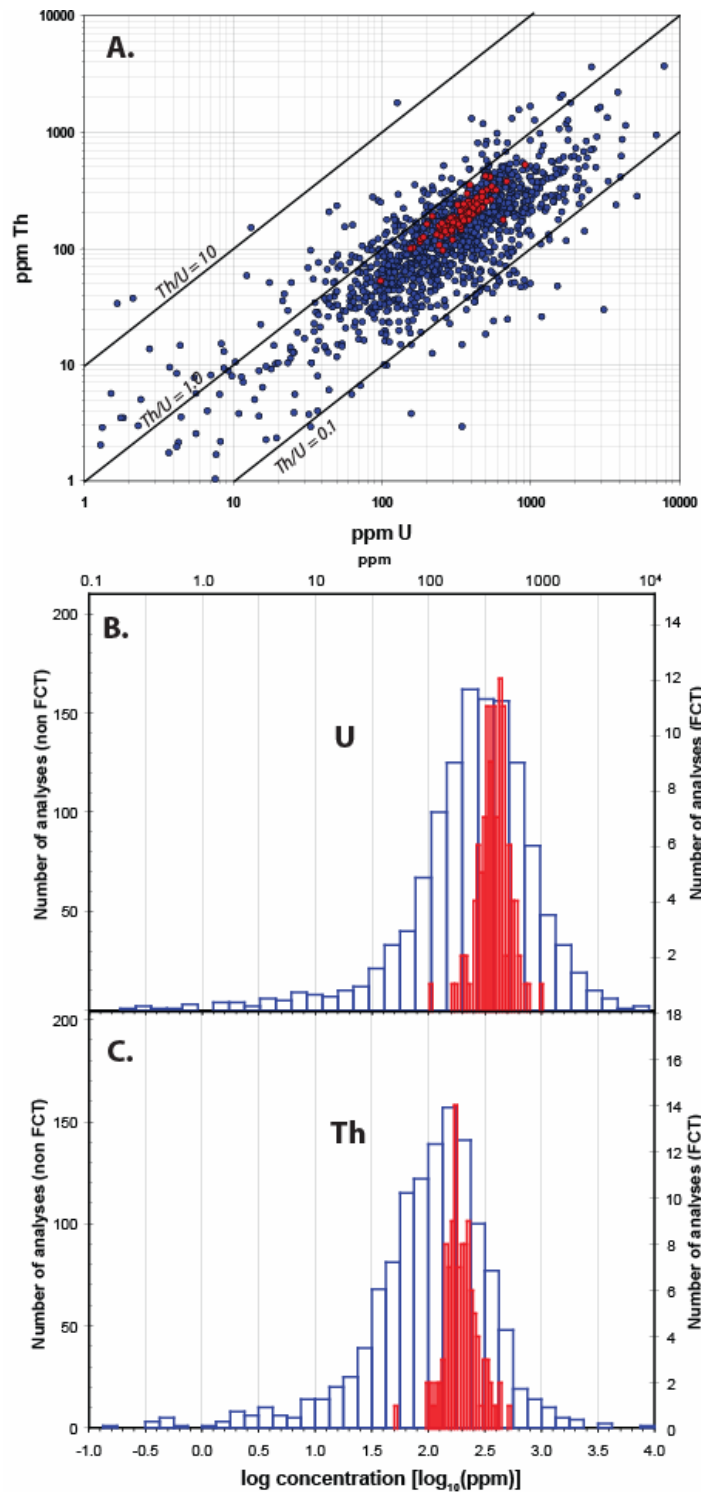


Figure 8. Concentrations of U and Th in dated zircons calculated from measured U and Th contents and estimated volumes and densities of dated crystals. Red: Fish Canyon Tuff zircon; blue: other samples. **A.** U versus Th concentrations. **B.,C.** Histograms of log U and log Th concentrations in zircon.

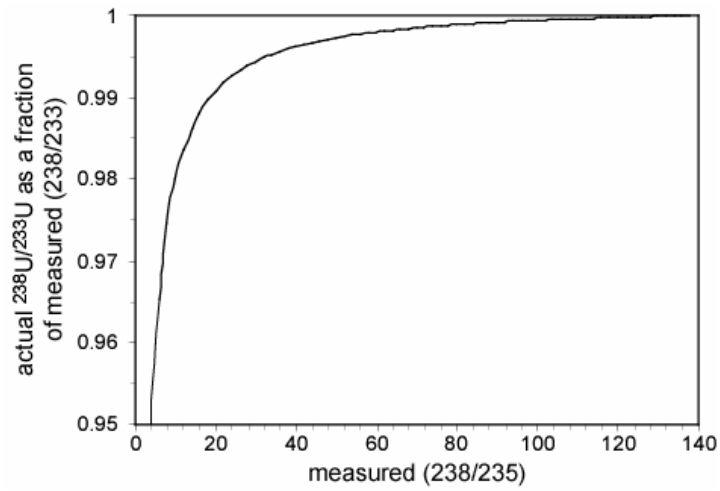


Figure 9. Correction factor for $^{238}\text{U}/^{233}\text{U}$ as a function of measured (238/233) and (238/235), assuming deviations in (238/235) are due to PtAr interference on U isotopes. Because ^{195}Pt is ~ 4.7 times more abundant than ^{198}Pt and ^{235}U is 138 times less abundant than ^{238}U , the measured (238/235) can be significantly different from the natural $^{238}\text{U}/^{235}\text{U}$ of 137.88, with little effect on the actual $^{238}\text{U}/^{233}\text{U}$ used to calculate U content of samples.

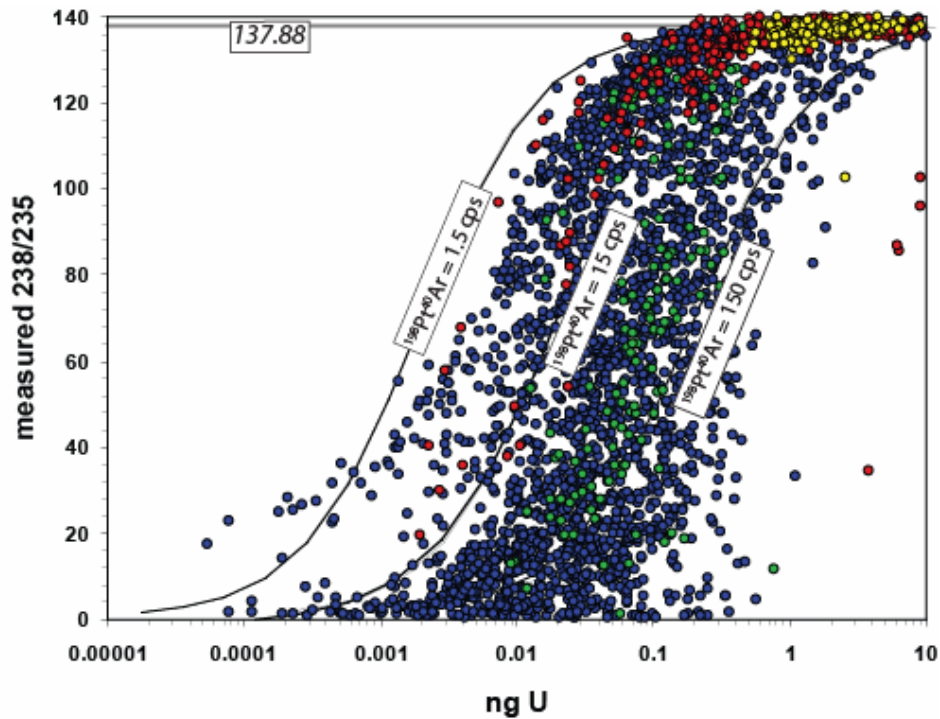


Figure 10. Measured (238/235) in dated apatite (blue circles; green circles are Durango) and zircon (red circles; yellow circles are FCT) aliquots, as a function of U content. At high U contents, the measured (238/235) is close to the natural U isotopic ratio of 137.88. At lower U contents, the measured (238/235) decreases because of the large interference of $^{195}\text{Pt}^{40}\text{Ar}$ on ^{235}U relative to that of $^{198}\text{Pt}^{40}\text{Ar}$ on ^{238}U . The low (238/235) at relatively high U for some zircons is attributed to incorporation of small amounts of Pt on crystals recovered from Pt foils used in He extraction, an obsolete method that has been replaced by the Nb foil method. Solid lines are predicted (238/235) for constant assumed intensities of 1.5, 15, and 150 cps at mass 238 from $^{198}\text{Pt}^{40}\text{Ar}$ (and proportional cps at mass 235 from $^{195}\text{Pt}^{40}\text{Ar}$) for different U contents (assuming a sensitivity of $1.5 \times 10^6/\text{ppb}$, and a standard sample volume of 3.0 ml).

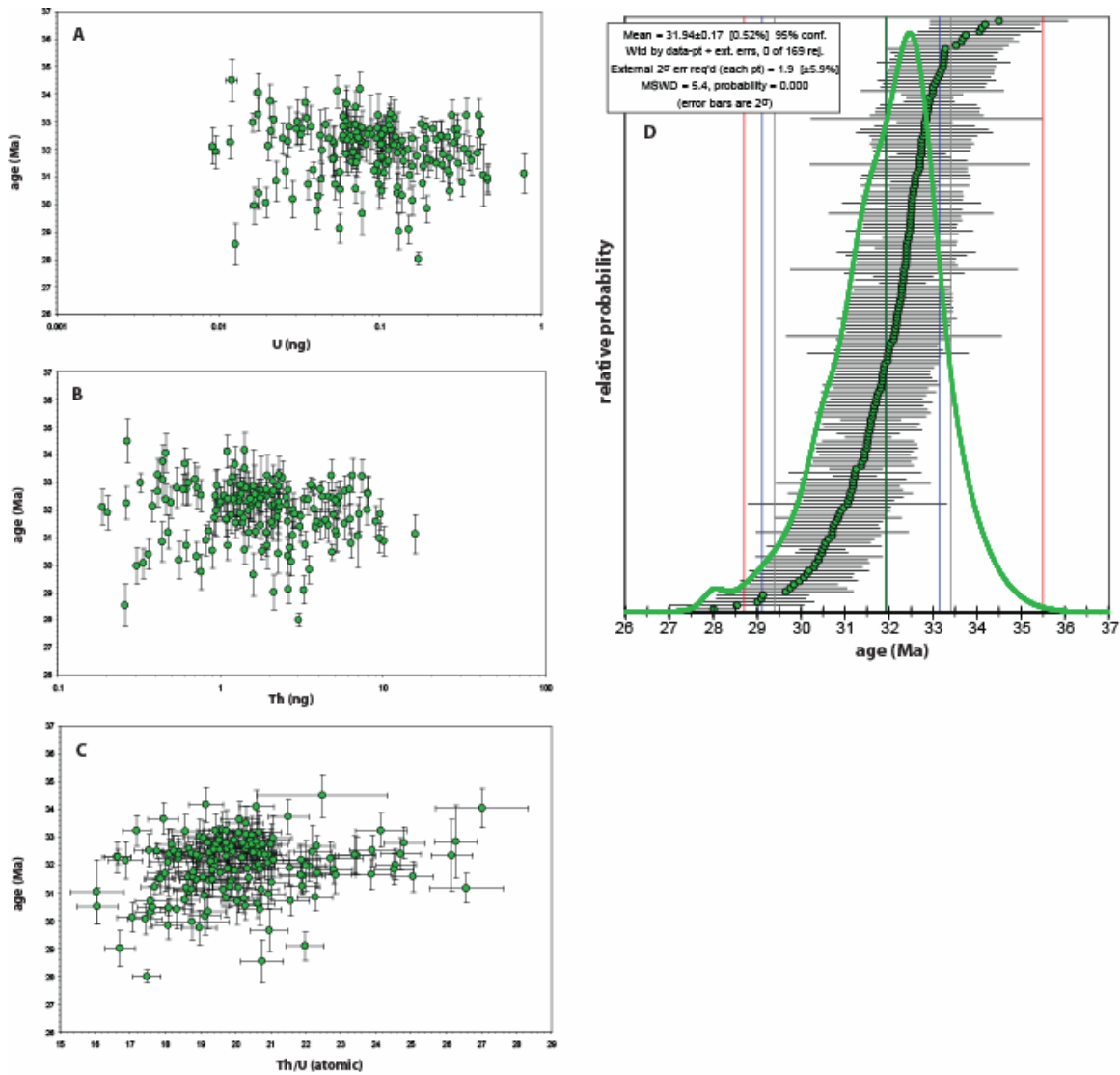


Figure 11. (U-Th)/He ages on 169 fragments from three different large gem-quality crystals of Durango apatite. **A** through **C** show ages plotted against masses of U and Th, and Th/U, with one-sigma analytical uncertainties (for most samples, error bars on U and Th masses are smaller than points). In panel **C**, one point at Th/U = 47 and age = 29.1 Ma is not shown. **D** is probability density and individual aliquot ages (arranged in order of increasing age) of the ages. Bold green vertical line is mean age of these aliquots. Other vertical lines represent ranges of two standard deviations of age replicates determined in other studies by: 1) laser-heating (U-Th)/He (red; House et al., 2000); 2) laser-heating (U-Th-Sm)/He (blue; McDowell et al., 2005); 3) apatite fission-track (grey; Jonckheere et al., 1993). About two-thirds of the Durango ages here include Sm measurements, which typically decreases ages by 0.3-0.5%. Statistics reported in panel **D** are from Isoplot 3.0 (Ludwig, 2003) and references therein.

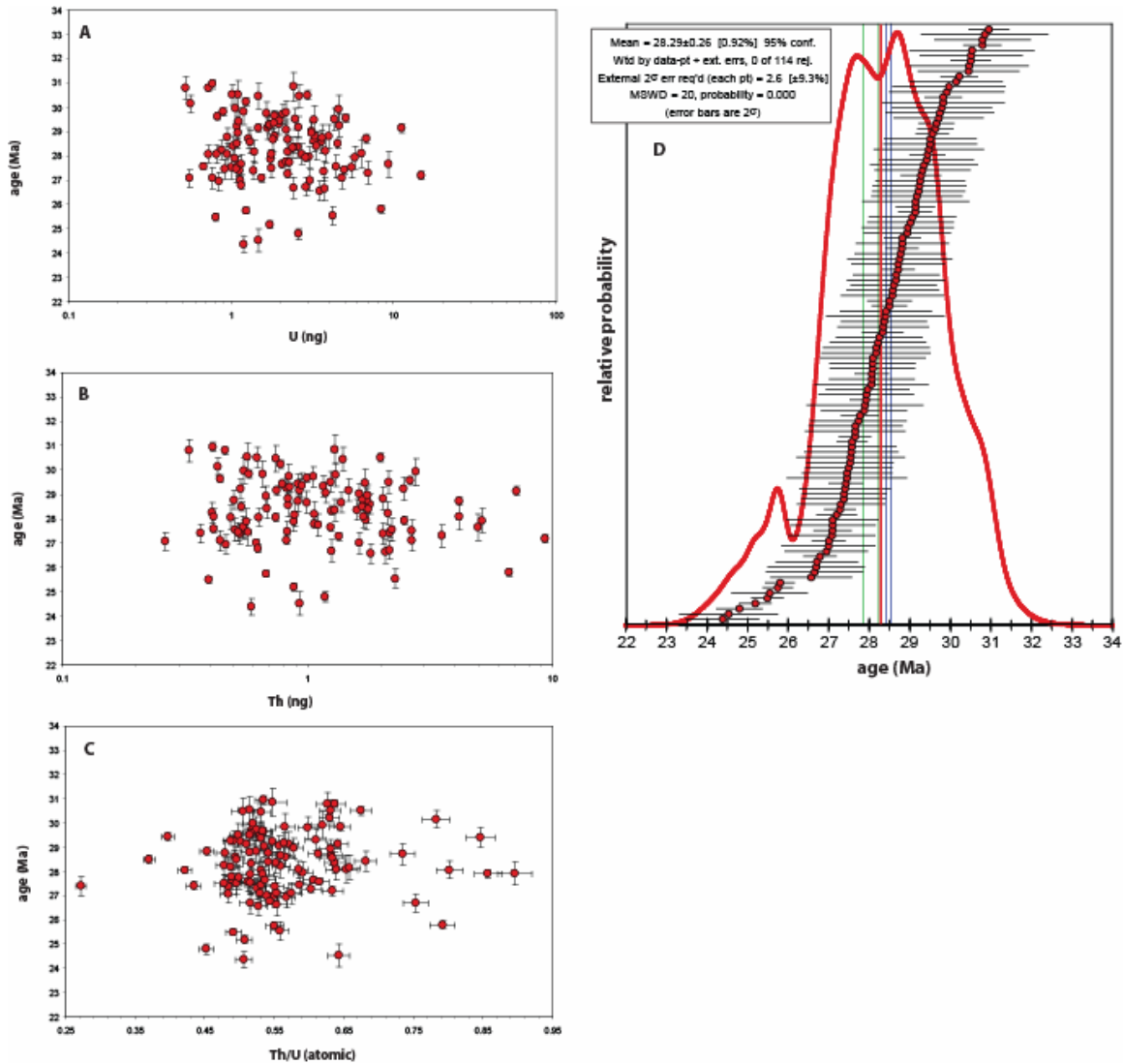


Figure 12. (U-Th)/He ages on 114 crystals of Fish Canyon Tuff zircon (two different whole rock samples generated these crystals). **A** through **C** show ages plotted against masses of U and Th, and Th/U, with one-sigma analytical uncertainties (for most samples, error bars on U and Th masses are smaller than points). **D** is probability density and individual crystal ages (arranged in order of increasing age) of the ages. Bold red vertical line is mean age of these aliquots. Other vertical lines represent 2σ or 95% confidence intervals for U/Pb TIMS ages of FCT zircons (Schmitz and Bowring, 2001) and ⁴⁰Ar/³⁹Ar ages of FCT sanidine (Renne et al., 1998). Statistics reported in panel **D** are from Isoplot 3.0 (Ludwig, 2003) and references therein. The higher standard deviation of this sample (and all typical crystals) relative to Durango apatite likely originates in errors associated with α-ejection correction, including the effects of heterogeneous intracrystalline distribution of U and Th.